Dual-Frequency Sweeping Light Source Based on Four-Wave Mixing in Silicon-on-Insulator Nano-Waveguide

Dun Qiao[a], Kang Li*[a], Sivagunalan Sivanathan [a], Bethan Copner [a], Nigel Copner [a], Michael Campbell[b], and Ben Hughes[b]

[a]Wireless and Optoelectronics Research and Innovation Centre, Faculty of Computing, Engineering and Science, University of South Wales, Cardiff, UK, CF37 1DL, [b]National Physical Laboratory, Hampton Road, Teddington, Middlesex, UK, TW11 0LW

*kang.li@southwales.ac.uk

ABSTRACT

Four-wave mixing (FWM) is a well-known technique to achieve all-optical control wavelength conversion. We propose a well-designed silicon nano-waveguide based on silicon-on-insulator (SOI) to achieve FWM conversion. Particularly, the original signal light continuously sweeps along the C band, and the generated idler light is correspondingly sweeping as the original signal is swept. The wavelengths of the idler and signal lights are symmetric with respect to the pump light wavelength. Simulation and experimental results of the FWM conversion properties are well-matched. With the pump light filtered out, a dual-frequency continuously sweeping laser source is achieved, which could be applied in dual-frequency scanning interferometry to eliminate dynamic errors in practical use.

Keywords: Four-wave mixing; silicon-on-insulator; nano-waveguide.

1. INTRODUCTION

The silicon material is ideal to be widely applied in photonics devices owning to its transparency at 1.3~1.7 μm wavelength range, high compatibility with the current complementary metal-oxide-semiconductor (CMOS) process [1], high refractive index (3.5 around 1.5 μm wavelength), and high non-linear refractive index [2]. SOI, a material comprised by placing a thin film of silicon on a layer of insulated silicon dioxide substrate, has been seen as the priority approach to minimize the scale of optical devices down to nanometer level and to significantly reduce energy consumption. In recent years, a series of optical devices has been achieved using the SOI material, including couplers [3, 4], tunable attenuators [5], optical switches [6] and modulators [7]. Among these devices, several optical non-linear effects were applied to achieve wavelength conversion and multiplication. In particular, the FWM as a third-order nonlinear process which generates a new frequency of light from the interaction of two or more incident lights in a non-linear medium, has been investigated and seen as one of the main approaches to wavelength conversion in silicon photonics [8, 9].

Frequency sweeping interferometry (FSI) is a technique for absolute distance measurement, which could be applied in many industries including large scale parts assembly (aero plane wing, shipbuilding) [10], robot arm calibration [11], and tiny deformation detection for structural analysis. However, FSI accuracy suffers from unwanted deliberate movement and vibration of both the target and sensing system. A Dual-frequency sweeping concept was proposed to overcome this problem and enhance FSI accuracy [12], however their accuracy is still limited by the optical light source tuning range. In this paper, we propose and demonstrate a laser system with dual-frequency sweeping, where one sweeps up and another

sweeps down symmetrically based on FWM on a SOI nano-waveguide. Both optical frequencies have a wide tuning range that covers the whole C band and is sufficient for FSI to achieve its own expected accuracy.

2. SIMULATION AND DESIGN OF SOI WAVEGUIDE

FWM only occurs when the phase-matching condition of two incident lights is satisfied [13], a generated light, or idler light, with wavelength λ_i is generated by the interaction between incident pump light λ_p and signal light λ_s, where $1/\lambda_i$ equals to $1/\lambda_p - 1/\lambda_s$ due to the energy conversion condition [14]. For our system, with a sweeping signal and a constant pump wavelength incident to the SOI waveguide, an idler light is generated. The wavelengths of the idler and

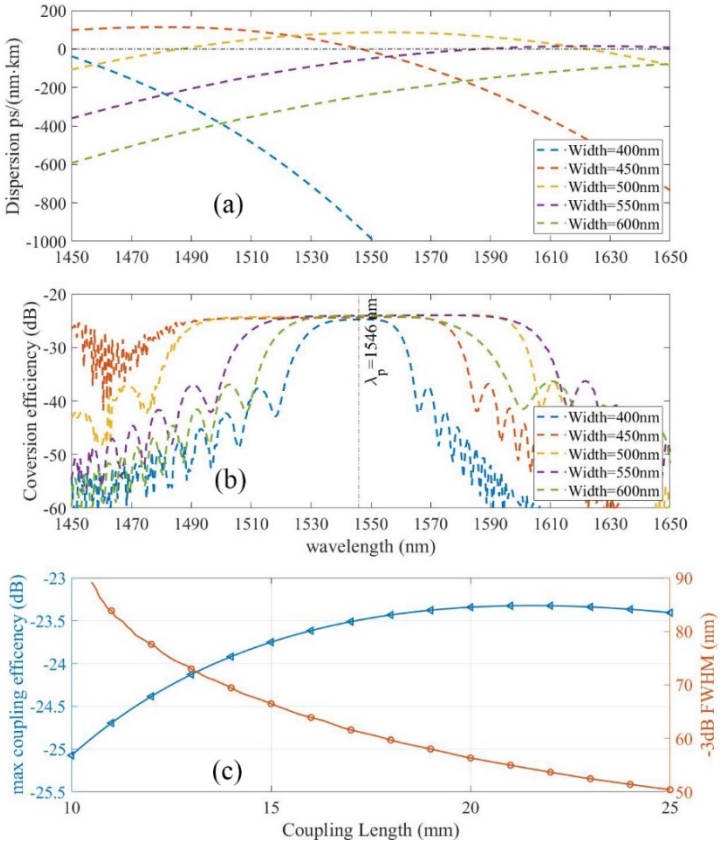

Figure 1. (a) The GVD of different width SOI waveguides with 220nm height. (b) the conversion efficiency of different width SOI waveguides with 220nm height, here the pump energy is 10 dBm, coupling length is 10 mm, pump wavelength is 1546 nm, and the 500 nm width (dotted yellow curve) shows the largest conversion band. (c) the maximum coupling efficiency decreases with the increase of coupling length, and the longer the length, the shorter the conversion band.

signal lights are symmetric with respect to the wavelength of pump light. Therefore, dual laser output with symmetrical sweeping could be achieved. The frequency tuning range in a FSI system is crucial for the measurement resolution and accuracy [15], therefore a wide tuning range laser is normally adopted as the source of the FSI system, which creates challenges in the design of the SOI waveguide to achieve broad FWM conversion bandwidth. Firstly, the frequency of generated idler light depends on the signal light, which is to achieve wideband dual sweeping, the FWM conversion band

should be wide enough. A generated idler light should have a comparable intensity to the signal light, which signifies the conversion efficiency should maintain acceptable levels along the whole tunning range.

The conversion bandwidth of FWM in SOI is highly dependent on the dispersion profile, which is dominated by the geometrical structure of the SOI waveguide. The dispersion profile β_n, of the order n, can be obtained from the derivative of the mode effective refractive index n_{eff} by the following equation [13]:

$$\beta = n_{eff}\omega, \omega = \frac{2\pi}{\lambda}, \beta_n = \frac{d^n\beta}{d\omega_n} \tag{1}$$

We simulated the mode profile and corresponding n_{eff} by a eigen mode solver based on a finite element analysis method supplied by COMSOL, the spectrums of group velocity dispersion (GVD) $D = -2\pi c\beta_2/{\beta_n}^2$ of waveguides with different width are shown in Fig. 1a, the height of the waveguide are all 220 nm since SOI wafer with 220 nm top layer is relatively easy to acquire. The waveguide with 500 nm (yellow curve) width has flattest dispersion curve along 1450 nm to 1650 nm, which indicates that 500 nm will show the best broadband conversion properties along this range. It is also notable that with increasing waveguide width, their dispersion spectrum shows a trend of red-shift and becomes relatively flat, this is because the dispersion sensitivity of the waveguide is reducing due to the reduction in energy density caused by the increased cross-sectional area of the waveguide.

With the dispersion profile, the conversion efficiency and band of FWM in silicon waveguide is then calculated. As mentioned previously, the FWM needs the phase-matching condition to be satisfied. With degenerated pump light, the mismatch Δk is expressed as:

$$\Delta k = 2\gamma P_{pump} - \Delta k_{linear} \tag{2}$$

The parameter $\gamma = 2\pi n_2/\lambda A_{eff}$ here is the non-linear coefficient, n_2 is the non-linear refractive index of the silicon, and for our simulation, we take $n_2 = 5.59 \times 10^{-18}\, m^2/W$ [16]. The pump wavelength λ_p is taken as 1545 nm and the effective area A_{eff} is calculated from the simulated mode profile function. P_{pump} is the power of pump wave and the parameter Δk_{linear} is the linear phase mismatch, which is relative to the dispersion at the wavelength of pump, signal, and idler light respectively. Since $1/\lambda_i = 1/\lambda_p - 1/\lambda_s$, the linear phase mismatch is then expressed as:

$$\Delta k_{linear} = \Delta\beta = -\beta_2(\Delta\omega)^2 - \frac{1}{12}\beta_4(\Delta\omega)^4 \tag{3}$$

With the phase mismatch obtained, the coupling wave equations [14] are solved by a customized MATLAB script to get the amplitude of pump, signal, and idler signal respectively.

$$\begin{cases} \dfrac{dA_p}{dL} = -\dfrac{1}{2}\left(\alpha_p + \alpha_{TPA_p} + \alpha_{FCA_p}\right)A_p + j\gamma_p\left[|A_p|^2 + 2|A_s|^2 + 2|A_i|^2\right]A_p \\ \qquad +2j\gamma_p A_p^* A_s A_c \exp(j\Delta kL) \\ \dfrac{dA_s}{dL} = -\dfrac{1}{2}(\alpha_s + \alpha_{TPA_s} + \alpha_{FCA_s})A_s + j\gamma_s\left[2|A_p|^2 + |A_s|^2 + 2|A_i|^2\right]A_s \\ \qquad +j\gamma_s A_c^* A_p^2 \exp(j\Delta kL) \\ \dfrac{dA_i}{dL} = -\dfrac{1}{2}(\alpha_i + \alpha_{TPA_i} + \alpha_{FCA_i})A_i + j\gamma_i\left[2|A_p|^2 + 2|A_s|^2 + |A_i|^2\right]A_i \\ \qquad +2j\gamma_c A_s^* A_p^2 \exp(j\Delta kL) \end{cases} \tag{4}$$

Where α, α_{TPA} and α_{FCA} are linear absorption, twin photons absorption (TPA), and free carrier absorption (FCA) coefficient respectively. The parameters A_p, A_s and A_i are the amplitude of the pump, signal, and idler respectively. L is the coupling length of the SOI waveguide. The conversion efficiency is then given by:

$$CE = \frac{{A_{idler}}^2}{{A_{signal}}^2} \tag{5}$$

Fig. 1b shows the conversion efficiency spectrum of waveguides with different width, and as predicted, the 500 nm width (yellow curve) waveguide displays the largest conversion band (~100 nm). Equation 4 also shows that the amplitudes of the different wave, or equivalently, the conversion efficiency, is derived from a function with respect to the coupling length L, so a sweeping simulation towards the coupling length is implemented, the result is shown in Fig. 1c, where the left axis and blue curve is the maximum conversion efficiency with varying length, and the right axis and red curve is the full width of half maximum of the conversion band along different coupling lengths. The pump energy and wavelength for the sweeping operation is set as 10 dBm and 1546 nm respectively. The results shows that the conversion efficiency will increase as the coupling length increased. However, the coupling length can't be infinitely long since the linear absorption is also enhanced by expanding the coupling length and the conversion efficiency will be reduced by continuously increasing linear absorption. Due to all three kinds of absorption effects, the conversion bandwidth decreases dramatically with increasing length, therefore, a trade-off between the conversion band and efficiency for practical application is inevitable.

Based on the simulation results, we take the 500 nm width and 220 nm height waveguide with 15 mm coupling length as our final design, since at this width the largest conversion band is obtained. 15 mm is selected under a trade-off with the wafer size, and this length could provide more chips on a single wafer, besides, the 15 mm coupling length still illustrates both acceptable conversion efficiency and bandwidth.

3. EXPERIMENTAL LAYOUT

Based on the design discussed in the last section, several batches of SOI waveguide were fabricated at Glasgow university and a testing system to evaluate the FWM properties of SOI waveguide was built at the University of South Wales.

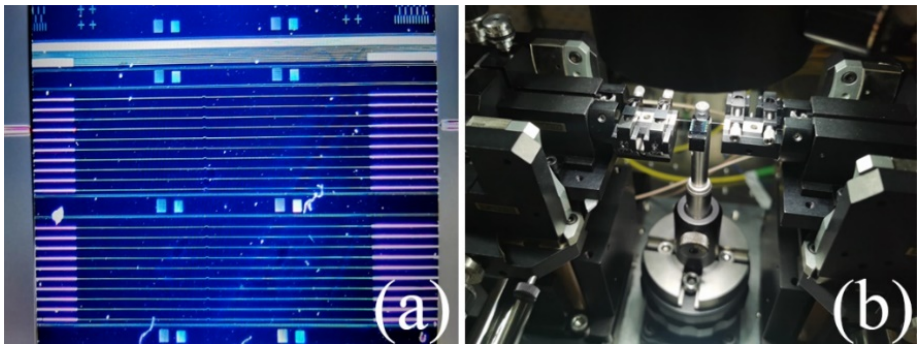

Figure 2. (a) microscope view of the SOI waveguide sample (b) lensed fiber alignment system for SOI waveguide

The FWM conversion efficiency is highly dependent on the pump energy, which means the input energy of the pump light into the waveguide must be as high as possible. The coupling from the waveguide to fiber or inverse has troubled many

researchers, for this design, we selected a taper coupler with SU-8 cladding that is fabricated at both sides of the SOI waveguides since it has been proven as a mature design [4]. As it can be seen in Fig. 2a, two groups of the waveguide are in view, each group contains 10 waveguides, the violet area at both ends of each waveguide has clearly bigger width than the silicon waveguide, which is the SU-8 cladding covering the tapered silicon waveguide. Our test indicated that for each side coupling, there is ~4 dBm insertion loss, which may be caused by many factors including the roughness of the SU-8 cladding, cleaving angle, and fabrication tolerance.

Fig. 3 is the block diagram of the SOI waveguide testing system. Both the FWM properties tests, and dual-frequency sweeping are conducted on this system. A Thorlabs DFB laser with a 1544 nm – 1546 nm tuning range is amplified with a 23 dBm erbium-doped fiber amplifier (EDFA) is used as the pump source, their light output will pass a short pass filter (<1545 nm) to eliminate the noise from the Amonic EDFA gain spectrum, which is mainly located over 1550 nm. A New Focus TLM-8700 tunable laser is employed at the signal source, and its output is also amplified by another 23 dBm EDFA and then passes through a 99/1 splitter, where 1% of the energy of the light is directed to a Mach Zehnder interferometer to generate the clock signal for FSI sampling synchronization. After that, a 90/10 splitter takes 90% of the signal light to a -3 dB coupler for recombination with the pump signal and then to the SOI waveguide for FWM, another 10% is guided to be recombined with the idler signal from FWM and then to be used for dual-frequency FSI. As it is shown in Fig. 2b, the SOI waveguide chip is placed on a fixed mount between two 6-axis adjustable fiber mounts with two lensed fibers for coupling in and out, respectively. A notch filter and a long pass filter are placed after the SOI, to eliminate the pump and signal light from the FWM output, after these two filters, only the idler light remained, which is then amplified by another 23 dBm EDFA to be combined with 10% of the original signal light, finally to be guided to the collimating lens of FSI system for illuminating the target. The schematic of the FSI module is not shown comprehensively since this paper is only focusing on the dual frequency sweeping laser source design.

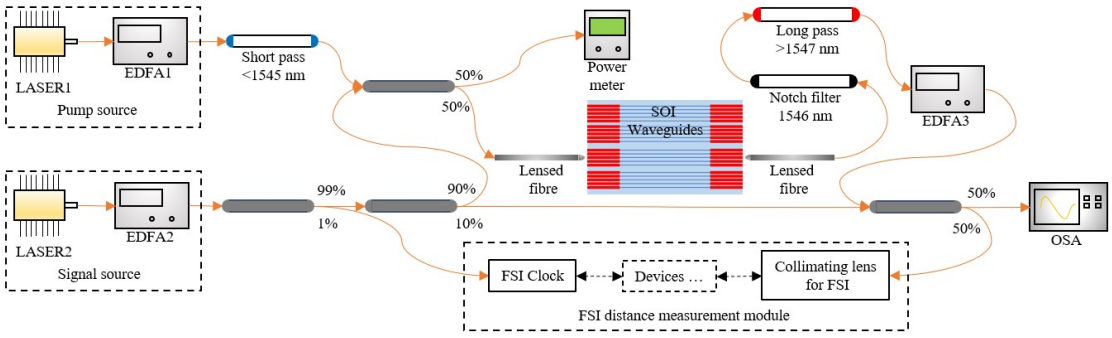

Figure 3. Block diagram of SOI waveguide testing system

4. RESULTS AND DISCUSSION

The sequence of testing started with FWM conversion efficiency for the silicon nano-waveguide, for this FWM conversion testing, the notch filter, long pass filter and 10% of the original signal are not required, the FWM output from the silicon waveguide through lensed fiber is directly linked to the OSA for analysis. Then, the dual-frequency laser output is tested, for that test, the filters and 10% of original signal light are required.

The wavelength detuning is introduced when describing the wavelength status of the conversion band and efficiency. The wavelength detuning is the difference of wavelength between pump and signal light, it is given by $\lambda_{detuning} = |\lambda_p - \lambda_s|$.

The tested conversion efficiency is given by the energy of idler light minus the energy of signal light, both energies are in dBm unit, the conversion efficiency is in dB units. Fig. 4a and 4b are the FWM spectrum of SOI waveguide with the smallest (1.32 nm) and largest (26.04 nm) tested wavelength detuning, respectively. At the smallest wavelength detuning point, the SOI waveguide shows good FWM conversion, not only the generated 1st order idler light (peak 4), the generated 2nd order FWM light is also clearly seen (the tiny peak at the right of peak 4). As it is shown in Fig. 4c, the tested conversion efficiency of SOI drops a little when the wavelength detuning exceeds 15 nm, because the conversion here is evaluated by the reading the data from the optical spectrum analyzer (OSA). When the detuning wavelength exceeds 15 nm, the sweeping band of OSA is required to be expanded to cover the range from signal to idler wavelength, since the sampling rate and step of the OSA will be influenced by the expanding spectrum measuring range, the conversion efficiency read from OSA of large wavelength detuning will be relatively smaller than its real value. The error during fabrication of the SOI may also contribute to this mismatch between the simulation and experimental results, the plasma-enhanced chemical vapor deposition (PECVD) fabricated silicon dioxide covering the top of waveguide may have a different refractive index to the index we adopted for the simulation. It is noticeable that the conversion efficiency of the largest wavelength detuning point is very high, which is higher than all the other sampling points. The reason behind this phenomenon is the influence

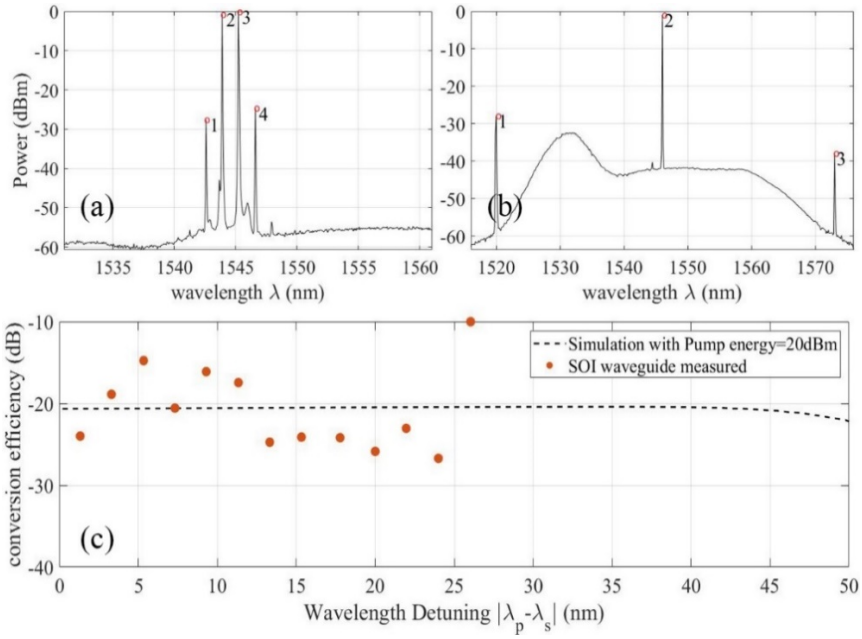

Figure 4. The experimental result of FWM on SOI waveguides with 500 nm, 220 nm height and 1.5 mm length, (a) the FWM spectrum at the smallest detuning point (1.32 nm) tested, where the peak 1,2,3 and 4 are converted pump, signal, Pump, and idler light respectively, (b) the FWM spectrum of at the largest detuning point (26.04 nm), where the peak 1,2, and 3 are signal, pump, and idler light respectively, the converted pump is out of the view since large detuning wavelength, (c) is the tested FWM conversion band of SOI.

of the EDFA's gain spectrum. Since the FWM is an energy sensitive process, both our pump light and signal light are pre-amplified by two EDFAs, which makes the results suffer from the EDFA gain spectrum, even though we applied a short pass filter to eliminate the influence of the EDFA's gain spectrum. As it is shown in Fig. 4b, both the signal and idler are

exceeding the gain band of the EDFA, which suggests the result at the largest wavelength detuning point is not comparable with the others, which concluded our testing process.

The simulation result indicates that the SOI waveguide with 500 nm width, 220 nm height, 1.5 mm length, and 20 dBm pump energy should have 50 nm detuning range, however, since the limitation of the EDFA gain band, the tested conversion efficiency of larger detuning wavelength is inaccessible, but based on the obtained results, the conversion efficiency keeps steady when the wavelength detuning reaches around 25 nm, which provides that the simulation results agree with the experimental results in for this investigation.

Then dual-frequency sweeping for FSI is tested. Fig.5 shows the dual sweeps generated by the silicon waveguide, as we mentioned in last section, the left peak (signal peak) is composed of 10% original signal light and long pass filtered signal light from FWM. At 20.8 nm detuning, the idler peak (-11.6956 dBm) of the SOI is still comparable with its signal peak (-6.6194 dBm), With the result shown, the dual-frequency sweeping laser output is achieved, it has 20.8 nm detuning range and pump wavelength at 1546 nm, which is equivalent as 1525.4 to 1567 nm tuning range, which is suitable enough to cover the whole C band, resulting in sufficient for dual-frequency FSI [12].

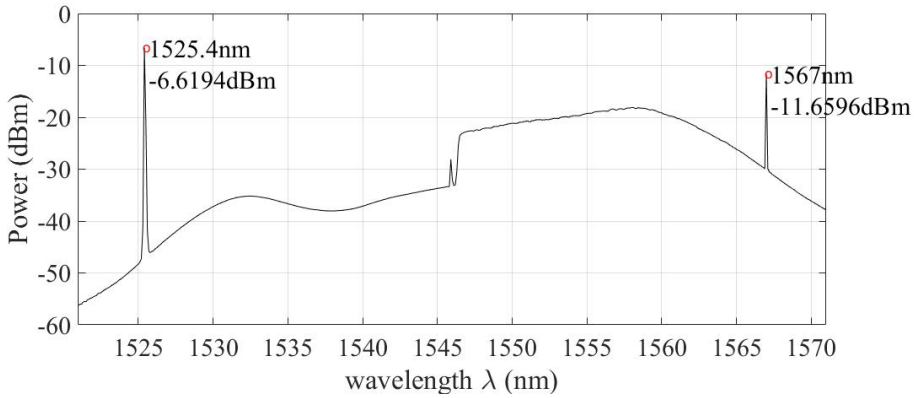

Figure 5. Dual sweeping generated by SOI waveguide. Left peak is the filtered signal light plus original signal light, and the right peak is the idler peak after EDFA 3. The detuning here is 20.8nm and the pump wavelength is 1546.2 nm

5. CONCLUSION

In this work, we investigate the effects of geometrical parameters of a SOI waveguide on the FWM conversion efficiency and bandwidth via numerical simulations, where a design supplying sufficient generated idler energy with continuously sweeping is achieved. The experimental results indicate that the proposed SOI waveguide can supply sufficient FWM conversion bandwidth and efficiency for achieving a dual-frequency symmetrically sweeping laser source with tuning range covering the whole C band. Particularly, this dual sweeping laser is suitable for a dual-frequency enhanced FSI distance measurement system. However, there are still some problems in this work, the insertion loss of the coupling from lensed fiber to the waveguide in this work is relatively high (~ -4 dBm), which needs to be addressed in the future work.

REFERENCES

[1] L. Chrostowski, and M. Hochberg, [Silicon photonics design: from devices to systems] Cambridge University Press, (2015).

[2] Q. Lin, O. J. Painter, and G. P. J. O. e. Agrawal, "Nonlinear optical phenomena in silicon waveguides: modeling and applications," 15(25), 16604-16644 (2007).

[3] D. Taillaert, P. Bienstman, and R. Baets, "Compact efficient broadband grating coupler for silicon-on-insulator waveguides," Optics letters, 29(23), 2749-2751 (2004).

[4] T. Tsuchizawa, K. Yamada, H. Fukuda *et al.*, "Microphotonics devices based on silicon microfabrication technology," IEEE Journal of selected topics in quantum electronics, 11(1), 232-240 (2005).

[5] K. Isamoto, K. Kato, A. Morosawa *et al.*, "A 5-V operated MEMS variable optical attenuator by SOI bulk micromachining," IEEE Journal of selected topics in quantum electronics, 10(3), 570-578 (2004).

[6] J. Song, Q. Fang, S. Tao *et al.*, "Fast and low power Michelson interferometer thermo-optical switch on SOI," Optics express, 16(20), 15304-15311 (2008).

[7] M. Nedeljkovic, S. Stanković, C. J. Mitchell *et al.*, "Mid-infrared thermo-optic modulators in SoI," IEEE Photonics Technology Letters, 26(13), 1352-1355 (2014).

[8] M. A. Foster, A. C. Turner, R. Salem *et al.*, "Broad-band continuous-wave parametric wavelength conversion in silicon nanowaveguides," Optics Express, 15(20), 12949-12958 (2007).

[9] Z. Wang, H. Liu, N. Huang *et al.*, "Impact of dispersion profiles of silicon waveguides on optical parametric amplification in the femtosecond regime," Optics express, 19(24), 24730-24737 (2011).

[10] C. Lu, G. Liu, B. Liu *et al.*, "Absolute distance measurement system with micron-grade measurement uncertainty and 24 m range using frequency scanning interferometry with compensation of environmental vibration," Optics express, 24(26), 30215-30224 (2016).

[11] K. Umetsu, R. Furutnani, S. Osawa *et al.*, "Geometric calibration of a coordinate measuring machine using a laser tracking system," Measurement science technology, 16(12), 2466 (2005).

[12] J. J. Martinez, M. A. Campbell, M. S. Warden *et al.*, "Dual-sweep frequency scanning interferometry using four wave mixing," IEEE Photonics Technology Letters, 27(7), 733-736 (2015).

[13] G. P. Agrawal, [Nonlinear fiber optics] Springer, (2000).

[14] S. Gao, Z. Li, Y. Xie *et al.*, "All-optical wavelength conversion based on four-wave mixing in silicon waveguides." 195-200.

[15] S. Sivanathan, M. A. Roula, N. J. Copner *et al.*, "Development of a Hardware for Frequency Scanning Interferometry for Long Range Measurement." 1-6.

[16] L. Zhang, A. M. Agarwal, L. C. Kimerling *et al.*, "Nonlinear Group IV photonics based on silicon and germanium: from near-infrared to mid-infrared," Nanophotonics, 3(4-5), 247-268 (2014).